C. R. Mecanique 344 (2016) 479–486

Contents lists available at ScienceDirect

Comptes Rendus Mecanique

www.sciencedirect.com

Analytical determination of the reflection coefficient by the evanescent modes model during the wave–current–horizontal plate interaction

Détermination analytique du coefficient de réflexion par le modèle des modes évanescents lors l'interaction houle–courant–plaque

Meriem Errifaiy, Smail Naasse, Chakib Chahine

Laboratory Physics of Polymers and Critical Phenomena, University Hassan II, Faculty of Science Ben M'sik Sidi Othman, P.B 7955 Casablanca, Morocco

ARTICLE INFO

Article history:
Received 6 January 2016
Accepted 11 March 2016
Available online 12 April 2016

Keywords:
Current
Regular wave
Evanescent modes
Reflection
Dispersion equation
Complex solutions

Mots-clés :
Courant
Houle
Modes évanescents
Réflexion
Équation de dispersion
Solutions complexes

ABSTRACT

Our work presents an analytical study of the determination of the reflection coefficient during the interaction between the regular wave current and a horizontal plate. This study was done using the linearized potential flow theory with the evanescent modes model, while searching for complex solutions to the dispersion equation that are neither real pure nor imaginary pure. To validate the established model, it has been confronted with the experimental results of V. Rey and J. Touboul, in a first phase, and then compared to those of the numerical study by H.-X. Lin et al. Then, this model was used to study the effect of current on the reflection coefficient.

RÉSUMÉ

On présente dans ce travail une étude analytique de la détermination du coefficient de réflexion lors de l'interaction houle–courant–plaque. Cette étude a été faite dans le cadre de la théorie potentielle linéarisée moyennant le modèle des modes évanescents, en cherchant des solutions complexes de l'équation de dispersion qui ne soient, ni réelles pures, ni imaginaires pures. Pour valider le modèle établi, on l'a d'abord confronté aux résultats expérimentaux de V. Rey et J. Touboul, puis à ceux, issus de la modélisation, de H.-X. Lin et al. Ensuite, on a utilisé ce modèle pour étudier l'effet du courant sur le coefficient de réflexion.

E-mail address: errifaiy.m@gmail.com (M. Errifaiy).

http://dx.doi.org/10.1016/j.crme.2016.03.004
1631-0721/

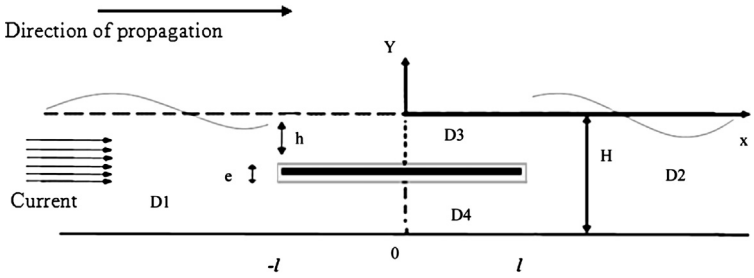

Fig. 1. Geometry of the problem.

1. Introduction

The protection of beaches, and of other coastal structures such as harbors, lakes etc. requires the maximization of wave reflection, hence the importance of wave reflectors. In certain circumstances, the wave is accompanied by currents. Wave reflectors, in these cases, have to consider the interaction wave–current.

The wave–current interaction has been the subject of several studies. We can name that by P. Osuna and J. Monbaliu in 2004 on the North Sea [1], the one by Y.-Y. Chen et al. in 2012 on the particle trajectory in Lagrangian description [2], and a theoretical and a numerical study by D. Zhifei and J.-T. Kirby on the interaction between a gravity wave of weak amplitude and a sheared current [3].

A submerged horizontal plate is a reflector of regular wave that enables the circulation of water, above and beneath; hence its environmental impact is minimal. In the last decades, the interaction between regular wave and plate has progressively attracted the interest of the researchers. In 1984, Patarapanich [4] showed, with the plane wave model, that the reflection coefficient of a gravity wave by a submerged horizontal plate depends on the ratio of the water depth to the wavelength of the incident wave, the ratio of the depth of the plate immersion to the depth of water, and on the ratio of the plate length to the wavelength of the wave that propagates above the plate. In 1986, Guevel [5] brought out that the body of water below the plate behaved as an oscillating wall. In 1990, H. Kojima et al. [6] presented an experimental study on energy transfer from the fundamental toward the transmitted second harmonic by the method of Goda using multiple probes. In 1993, Molin and Betous [7], to minimize the efforts on the structure, used a perforated tile and made an experimental and analytical study on the reflection coefficient, using the evanescent modes model. In 2001, Brossard et al. [8] showed experimentally, using a mobile probes technique, that during the interaction between a regular wave and plate, there is free upper harmonic production. In 2012, K. Wang et al. [9] presented an analysis of the velocity field using a numerical method (BEM). In 2014, H. Behera and T. Sahoo [10] studied the interaction of a gravity wave and of a flexible porous horizontal plate.

In 2003, V. Rey et al. [11] conducted an experimental study on wave–current–plate interaction for regular and irregular waves. In 2014, H.-X. Lin et al. [12] made a numerical study on the wave reflection and production of harmonics during the current–wave–plate interaction.

In this work, we present an analytical study of the determination of the reflection coefficient during the regular wave–current–plate interaction. This study was carried out as part of the linearized potential flow theory using the evanescent modes model. To take account of evanescent modes in the presence of current, the dispersion equation had to be solved by looking for complex solutions that are, neither pure real, nor pure imaginary.

To validate the established model, it has been confronted with the experimental results of V. Rey and J. Touboul [13], in a first phase, and then compared to those of the numerical study by H.-X. Lin et al. Then, this model was used to study the effect of current on the reflection coefficient.

2. Formulation of the problem

We are interested in the calculation of the reflection coefficient of a regular wave in the presence of uniform current, when interacting with a fixed horizontal plate totally immersed in a channel. The studied regular wave is potential and of low wave steepness, whereas the surface tension is negligible. A monochromatic wave is emitted upstream, and downstream, the wave does not undergo any reflection. The area of study is divided into four sub-domains, as shown in Fig. 1.

Seeking for the potential in the form of a superposition of potential associated with the current $\phi_c(x, y, t) = Ux$ and that associated with a monochromatic regular wave $\phi_h(x, y, t) = \varphi(x, y)e^{i\omega t}$, the total potential is written:

- in sub domains D_p, $1 \le p \le 3$:

$$\phi_p(x, y, t) = Ux + \left[A_p e^{ik_p^- x}\cosh\left(k_p^-(y + H_p)\right) + B_p e^{ik_p^+ x}\cosh\left(k_p^+(y + H_p)\right)\right]e^{i\omega t} + \left[\sum_{n=1}^{N}\left(A_{pn}e^{k_{pn}^- x}\cos\left(k_{pn}^-(y + H_p)\right) + B_{pn}e^{k_{pn}^+ x}\cos\left(k_{pn}^+(y + H_p)\right)\right)\right]e^{i\omega t} \quad (1)$$

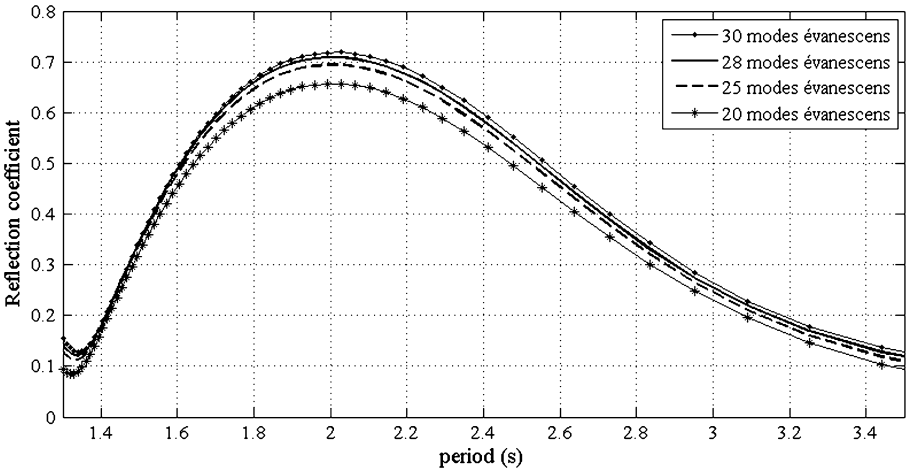

Fig. 2. Reflection coefficient as a function of the period for the following characteristics: plate thickness $e = 0.1$ m, plate length $2l = 1.53$ m, plate immersion $h = 0.5$ m, water depth $H = 3$ m and current velocity $U = 0.3$ m/s.

In this equation, H_1 and H_2 are both equal to the water depth in the channel ($H_1 = H_2 = H$), H_3 is equal to the plate immersion ($H_3 = h$), ω is the pulsation of the wave, N denotes the number of evanescent modes, A_{1n} and B_{2n} are all zero, A_1 is given by: $A_1 = g a_i \frac{1}{(\omega - U k_1^-)\cosh(k_1^- H)}$ (where a_i is the wave amplitude that propagates at the free surface, g is the acceleration of gravity), and the constants $k_p^{\pm}$ and $k_{pn}^{\pm}$ are the roots of the following equations, respectively:

$$\left(\omega \pm U\left(k_p^{\pm}\right)\right)^2 = g\left(k_p^{\pm}\right) \times \tanh\left(\left(k_p^{\pm}\right) H_p\right) \tag{2}$$

$$\left(\mathrm{i}\omega \pm U\left(k_{pn}^{\pm}\right)\right)^2 = g\left(k_{pn}^{\pm}\right) \times \tan\left(\left(k_{pn}^{\pm}\right) H_p\right) \tag{3}$$

- in sub domain D_4:

$$\phi_4(x, y, t) = Ux + \left[\left(A_4 + B_4 x + \sum_{n=1}^{N}\left(A_{4n}\mathrm{e}^{-\mu_n x} + B_{4n}\mathrm{e}^{\mu_n x}\right)\cos\left(\mu_n (y + H)\right)\right)\right]\mathrm{e}^{\mathrm{i}\omega t} \tag{4}$$

$$\mu_n = \frac{n\pi}{H - h - e} \quad \text{where } e \text{ is the plate's thickness.}$$

All constants $\{B_1, B_{1n}, A_3, B_3, A_{3n}, B_{3n}, A_4, B_4, A_{4n}, B_{4n}, A_2$ and A_{2n} for $1 \le n \le N\}$ that are present in the equations (1) and (4) are unknown.

The solutions to Eq. (2) are the wave numbers of the propagating modes. This equation has been subject of investigation of several studies. We can mention the study by P. Maissa et al. [14] and the experimental display by P. Faltot et al. [15].

The solutions to Eq. (3) correspond to evanescent modes. In the absence of current ($U = 0$), these solutions are pure real. However, in the presence of current, it is easy to verify that this equation firstly has no pure real solution, secondly the pure imaginary solutions are those corresponding to Eq. (2). Therefore, to establish this model, it is necessary to look for solutions ($k_{pn}^{\pm}$) to the nonzero real part and to the nonzero imaginary part, as well. Those solutions have to be such that $k_{pn}^- = -k_{pn}^+$.

By means of the matching conditions between the sub domains that express the continuity of the velocity potential and, that of the horizontal velocity at the edges of attack and trailing, of the plate ($x = -l$ and $x = l$, respectively), we obtain a linear algebraic system of $6N + 6$ equations and $6N + 6$ unknowns (see Appendix A). The wave reflection coefficient that propagates at the free surface is given by:

$$R = \frac{(\omega + U k_1^+)}{(\omega - U k_1^-)} \times \frac{\cosh(k_1^+ H)}{\cosh(k_1^- H)} \times \frac{B_1}{A_1}$$

The reflection coefficient, like the elements of the matrix corresponding to this system, depends on the relative depth kH (which expresses the ratio of the water depth in the channel to the wavelength of the incident wave, in the absence of current), on the plate immersion ratio (h/H), on the relative plate length ($2l$)/h (ratio of the total length of the plate at its immersion depth below the free surface level at rest) and on the Froude number ($U/\sqrt{gH}$).

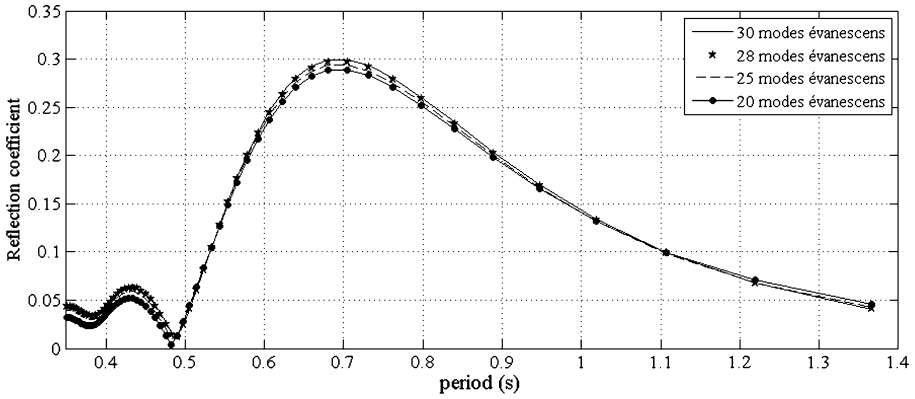

Fig. 3. Reflection coefficient as a function of the period for the following characteristics: plate thickness $e = 0.01$ m, plate length $2l = 0.25$ m, water depth $H = 0.2$ m, and relative current velocity $(U/C_{g0}) = 0.12$ (C_{g0} is the group velocity at $T = 0.75$ s) for a plate immersion at $h = 0.1$ m.

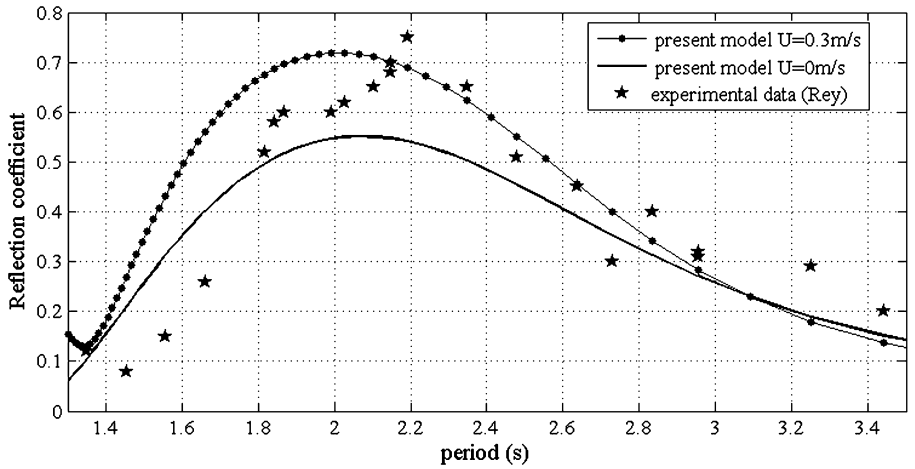

Fig. 4. Reflection coefficients as a function of the period for the following characteristics: plate thickness $e = 0.1$ m, plate length $2l = 1.53$ m, plate immersion $h = 0.5$ m, water depth $H = 3$ m, and current velocities $U = 0$ and 0.3 m/s.

3. Validation of the model

To validate this model, the results were compared with those made experimentally by V. Rey and J. Touboul [13] firstly, and then with the numerical results of H.-X. Lin et al. [12]. For each of these two cases, we studied the effect of the number N of evanescent modes taken into account in Eqs. (1) and (4). For this, the reflection coefficient calculated by this model is represented as a function of the period, for different values of the number N of evanescent modes. In Fig. 2, the reflection coefficient is calculated by using the data used by V. Rey and J. Touboul [13]. In Fig. 3, the data used are those of H.-X. Lin et al. [12].

The results in Figs. 2 and 3 show that the reflection coefficient calculated by this model increases with the number of evanescent modes taken into account. However when this number reached 28 the reflection coefficient cease to increase practically. For the rest, the number of evanescent modes taken into account is $N = 30$.

Fig. 4 shows, depending on the period, the values of the reflection coefficient measured experimentally by V. Rey and J. Touboul [13] and calculated analytically by this model. The analytical calculations were made in the absence of current ($U = 0$) and in the presence of a current of velocity $U = 0.3$ m/s, for a plate thickness $e = 0.1$ m.

Fig. 5 shows the values of the reflection coefficient, depending on the period, for $(U/C_{g0}) = 0.12$ (ratio of the current velocity relative to the (C_{g0}) group velocity calculated in the absence of current). The results of this model are compared with those calculated numerically by H.-X. Lin et al. [12].

In Fig. 6, we compare the results of this model with the results calculated numerically by H.-X. Lin et al. [12], by representing the values of the reflection coefficient as a function of the plate length, for $(U/C_{g0}) = 0.07$ (ratio of the current velocity relative to the (C_{g0}) group velocity calculated in the absence of current).

The results presented in Figs. 4–6 show that: (1) the results of this model are in agreement with the experimental values obtained by V. Rey and J. Touboul [13] and also with the numerical results of H.-X. Lin et al. [12]; (2) the model presents a slight difference in the range of periods between 1.5 and 2 s in comparison with the experimental results of V. Rey and J. Touboul [13].

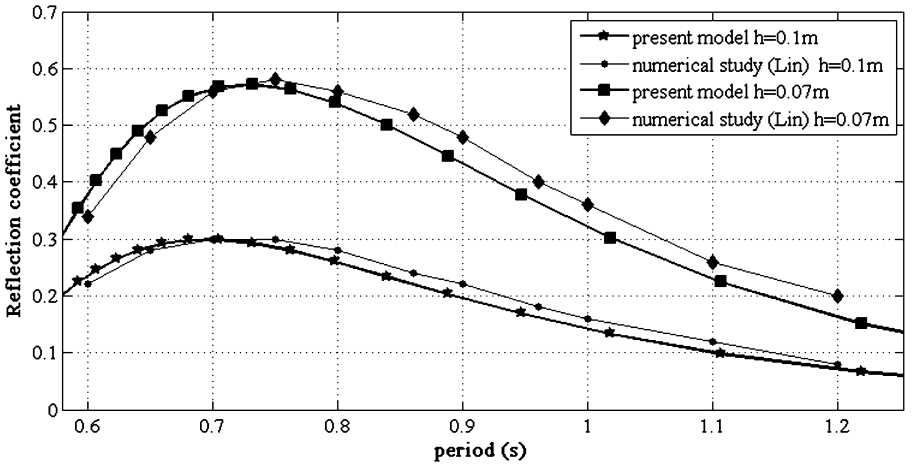

Fig. 5. Reflection coefficient as a function of the period for the following characteristics: plate thickness $e = 0.01$ m, plate length $2l = 0.25$ m, water depth $H = 0.2$ m, and relative current velocity $(U/C_{g0}) = 0.12$ (C_{g0} is the group velocity at $T = 0.75$ s) for plate immersions $h = 0.1$ m and $= 0.07$ m.

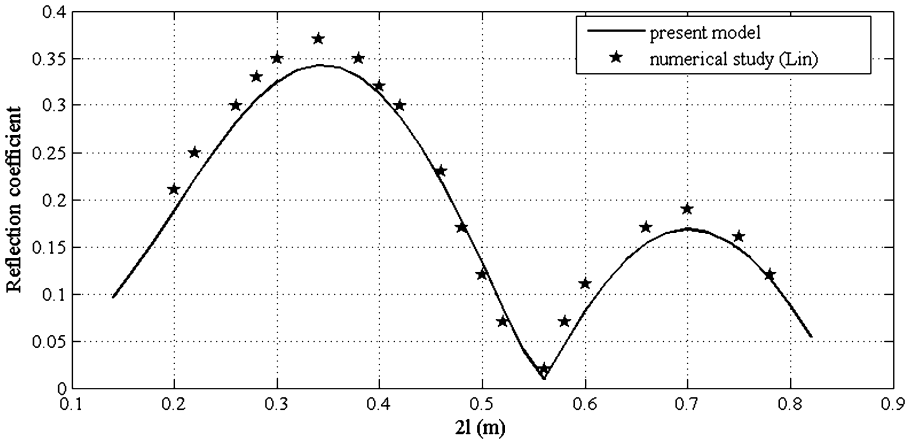

Fig. 6. Reflection coefficient as a function of the length of the plate, for: plate thickness $e = 0.01$ m, plate immersion $h = 0.1$ m, water depth $H = 0.2$ m, and relative current velocity $(U/C_{g0}) = 0.07$ (C_{g0} is the group velocity at $T = 0.75$ s).

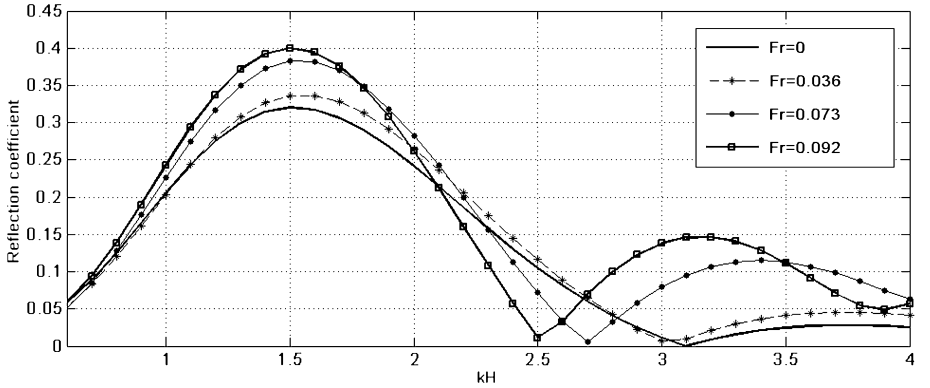

Fig. 7. Reflection coefficient as a function of kH for: a thin plate ($e = 0$) of relative plate length $2l/h = 3$, a plate immersion ratio $h/H = 0.5$, and different values of the Froude number ($Fr = \frac{U}{\sqrt{gH}}$).

4. Effect of the current

To study the effect of the current on the reflection coefficient of regular waves, the reflection coefficient was calculated by this theoretical model for different values of the Froude number while keeping constant the plate immersion ratio as

Table 1
Effect of the Froude number on the maximum of the reflection coefficient. M_0: reflection coefficient maximum calculated by this model without current. M: reflection coefficient maximum calculated by this model in the presence of current.

	Froude number		
	$\frac{U}{\sqrt{gH}} = 0.036$	$\frac{U}{\sqrt{gH}} = 0.073$	$\frac{U}{\sqrt{gH}} = 0.092$
$\frac{M-M_0}{M_0}$	5%	19.62%	24.84%

well as a relative plate length. Fig. 7 shows the variations of the reflection coefficient as a function of the relative depth (kH), for different values of the Froude number, ($\frac{U}{\sqrt{gH}} = 0$, $\frac{U}{\sqrt{gH}} = 0.036$, $\frac{U}{\sqrt{gH}} = 0.073$, $\frac{U}{\sqrt{gH}} = 0.092$). In Table 1, we present the relative difference of the reflection coefficient maximum ($\frac{M-M_0}{M_0}$, where M_0 is the reflection coefficient maximum in the absence of current and M is the reflection coefficient maximum in the presence of current) for the different values of the Froude number.

The results show that when the plate immersion ratio and relative plate length are both given: (1) the maximum of the reflection coefficient increases with the Froude number (2) the band with, where the reflection coefficient exceeds 0.25, increases slightly with the Froude number.

5. Conclusion

The evanescent modes model based on complex solutions to the dispersion equation, of non-zero real part and non-zero imaginary part, is consistent with the experimental measurements made by V. Rey and J. Touboul [13] as well as with the results of the numerical study by H.-X. Lin et al. [12].

By means of this model, we can deduce that (1) the maximum of the reflection coefficient increases with the Froude number, and (2) the band width where the reflection coefficient exceeds 0.25 increases slightly with the Froude number.

Appendix A

- The continuity of the velocity potential at the edge of attack ($x = -l$):

$$\phi_1(-l, y) = \phi_3(-l, y) \quad \text{if } h \le y \le 0$$
$$\phi_1(-l, y) = \phi_4(-l, y) \quad \text{if } H \le y \le -h$$

Multiplying these two equations respectively by $\cos(k_{3n}^{-}(y+h))$ and $\cos(\mu_n(y+H))$ then after integrating, we obtain:

$$\int_{-h}^{0} \phi_1(-l, y)\cos\big(k_{3n}^{-}(y+h)\big)\mathrm{d}y = \int_{-h}^{0} \phi_3(-l, y)\cos\big(k_{3n}^{-}(y+h)\big)\mathrm{d}y \quad (1 \le n \le N)$$
$$\int_{-H}^{-h} \phi_1(-l, y)\cos\big(\mu_n(y+H)\big)\mathrm{d}y = \int_{-H}^{-h} \phi_4(-l, y)\cos\big(\mu_n(y+H)\big)\mathrm{d}y \quad (1 \le n \le N)$$

This gives $2N$ equations (two equations for each value of n). Two other equations are obtained by replacing $\cos(k_{3n}^{-}(y+h))$ by $\cosh(k_3^{-}(y+h))$ and $\cos(\mu_n(y+H))$ by 1 (one) in the previous process, respectively. Hence the number of equations is $2N+2$.

- The continuity of the horizontal velocity at the edge of attack, ($x = -l$):

$$\frac{\partial\phi_1(-l, y)}{\partial x} = \frac{\partial\phi_3(-l, y)}{\partial x} \quad \text{if } h \le y \le 0$$
$$\frac{\partial\phi_1(-l, y)}{\partial x} = \frac{\partial\phi_4(-l, y)}{\partial x} \quad \text{if } H \le y \le -h$$

By multiplying these two equations by $\cos(k_{1n}^{+}(y+H))$ and then by integrating and summing, we obtain:

$$\int_{-H}^{0} \frac{\partial\phi_1(-l, y)}{\partial x}\cos\big(k_{1n}^{+}(y+H)\big)\mathrm{d}y = \int_{-h}^{0} \frac{\partial\phi_3(-l, y)}{\partial x}\cos\big(k_{1n}^{+}(y+H)\big)\mathrm{d}y$$

$$+\int_{-H}^{-h}\frac{\partial\phi_4(-l,y)}{\partial x}\cos\big(k_{1n}^{+}(y+H)\big)\mathrm{d}y\quad(1\le n\le N)$$

By replacing $\cos(k_{1n}^{+}(y+H))$ by $\cosh(k_{1}^{+}(y+H))$ in the previous process, we obtain another equation. In addition, by using the matching conditions between the sub domains at the edge of attack, we obtain $3N+3$ equations.

- By a similar process at the edge of trailing ($x=l$), by replacing ϕ_1 by ϕ_2, k_1^{+} by k_1^{-}, k_{1n}^{+} by k_{1n}^{-}, k_3^{-} by k_3^{+} and k_{3n}^{-} by k_{3n}^{+}, we obtain $3N+3$ other equations.

Therefore, using the continuity of the velocity potential and that of the horizontal velocity at the edges of attack and trailing of the plate, we obtain the following system (Eqs. (5)–(16)):

$$\int_{-h}^{0}\phi_1(-l,y)\cos\big(k_{3n}^{-}(y+h)\big)\mathrm{d}y=\int_{-h}^{0}\phi_3(-l,y)\cos\big(k_{3n}^{-}(y+h)\big)\mathrm{d}y\quad(1\le n\le N)\tag{5}$$

$$\int_{-h}^{0}\phi_1(-l,y)\cosh\big(k_{3}^{-}(y+h)\big)\mathrm{d}y=\int_{-h}^{0}\phi_3(-l,y)\cosh\big(k_{3}^{-}(y+h)\big)\mathrm{d}y\tag{6}$$

$$\int_{-H}^{-h}\phi_1(-l,y)\cos\big(\mu_n(y+H)\big)\mathrm{d}y=\int_{-H}^{-h}\phi_4(-l,y)\cos\big(\mu_n(y+H)\big)\mathrm{d}y\quad(1\le n\le N)\tag{7}$$

$$\int_{-H}^{-h}\phi_1(-l,y)\mathrm{d}y=\int_{-H}^{-h}\phi_4(-l,y)\mathrm{d}y\tag{8}$$

$$\int_{-H}^{0}\frac{\partial\phi_1(-l,y)}{\partial x}\cos\big(k_{1n}^{+}(y+H)\big)\mathrm{d}y=\int_{-h}^{0}\frac{\partial\phi_3(-l,y)}{\partial x}\cos\big(k_{1n}^{+}(y+H)\big)\mathrm{d}y+\int_{-H}^{-h}\frac{\partial\phi_4(-l,y)}{\partial x}\cos\big(k_{1n}^{+}(y+H)\big)\mathrm{d}y\quad(1\le n\le N)\tag{9}$$

$$\int_{-H}^{0}\frac{\partial\phi_1(-l,y)}{\partial x}\cosh\big(k_{1}^{+}(y+H)\big)\mathrm{d}y=\int_{-h}^{0}\frac{\partial\phi_3(-l,y)}{\partial x}\cosh\big(k_{1}^{+}(y+H)\big)\mathrm{d}y+\int_{-H}^{-h}\frac{\partial\phi_4(-l,y)}{\partial x}\cosh\big(k_{1}^{+}(y+H)\big)\mathrm{d}y\tag{10}$$

$$\int_{-h}^{0}\phi_2(l,y)\cos\big(k_{3n}^{+}(y+h)\big)\mathrm{d}y=\int_{-h}^{0}\phi_3(l,y)\cos\big(k_{3n}^{+}(y+h)\big)\mathrm{d}y\quad(1\le n\le N)\tag{11}$$

$$\int_{-h}^{0}\phi_2(l,y)\cosh\big(k_{3}^{+}(y+h)\big)\mathrm{d}y=\int_{-h}^{0}\phi_3(l,y)\cosh\big(k_{3}^{+}(y+h)\big)\mathrm{d}y\tag{12}$$

$$\int_{-H}^{-h}\phi_2(l,y)\cos\big(\mu_n(y+H)\big)\mathrm{d}y=\int_{-H}^{-h}\phi_4(l,y)\cos\big(\mu_n(y+H)\big)\mathrm{d}y\quad(1\le n\le N)\tag{13}$$

$$\int_{-H}^{-h}\phi_2(l,y)\mathrm{d}y=\int_{-H}^{-h}\phi_4(l,y)\mathrm{d}y\tag{14}$$

$$\int_{-H}^{0} \frac{\partial\phi_2(l,y)}{\partial x}\cos\big(k_{1n}^{-}(y+H)\big)\mathrm{d}y = \int_{-h}^{0} \frac{\partial\phi_3(l,y)}{\partial x}\cos\big(k_{1n}^{-}(y+H)\big)\mathrm{d}y + \int_{-H}^{-h} \frac{\partial\phi_4(l,y)}{\partial x}\cos\big(k_{1n}^{-}(y+H)\big)\mathrm{d}y \quad (1\le n\le N) \tag{15}$$

$$\int_{-H}^{0} \frac{\partial\phi_2(l,y)}{\partial x}\cosh\big(k_{1}^{-}(y+H)\big)\mathrm{d}y = \int_{-h}^{0} \frac{\partial\phi_3(l,y)}{\partial x}\cosh\big(k_{1}^{-}(y+H)\big)\mathrm{d}y + \int_{-H}^{-h} \frac{\partial\phi_4(l,y)}{\partial x}\cosh\big(k_{1}^{-}(y+H)\big)\mathrm{d}y \tag{16}$$

This is a linear algebraic system of $6N+6$ equations and $6N+6$ unknowns, which are the constants $\{B_1, B_{1n}, A_3, B_3, A_{3n}, B_{3n}, A_4, B_4, A_{4n}, B_{4n}, A_2$ and A_{2n} for $1\le n\le N\}$. The linearity of this system results from that of the velocity potential. The elements of the matrix corresponding to this system depend on h, H, $2l$, ω, and U. The wave pulsation ω is depending on kH by means of the dispersion equation in absence of current $\frac{\omega^2 H}{g} = kH \times \tanh(kH)$, where k is the wave number of the incident wave in the absence of current. Hence the elements of the matrix corresponding to this system depend on kH, h/H, $2l/h$, and $U/\sqrt{gH}$.

References

[1] P. Osuna, J. Monbaliu, Wave–current interaction in the Southern North Sea, J. Mar. Syst. 52 (2004) 65–87.
[2] Y.-Y. Chen, H.-C. Hsu, H.-H. Hwung, Particle trajectories beneath wave–current interaction in a two-dimensional field, Nonlinear Process. Geophys. 19 (2012) 185–197.
[3] Z. Dong, J.-T. Kirby, Theoretical and numerical study of wave–current interaction in strongly-sheared flows, in: Proc. 33rd Int. Conf. Coastal Engrng., Santander, Spain, 2012.
[4] M. Patarapanich, Maximum and zero reflection from submerged plate, J. Waterw. Port Coast. Ocean Eng. 110 (1984) 171–181.
[5] P. Guevel, E. Landel, R. Bouchet, J.-M. Manzone, Le phénomène du mur d'eau oscillant et son application pour protéger un site côtier soumis à la houle, in: Permanent International Association of Navigation Congresses, 1986.
[6] H. Kojima, T. Ijima, A. Yshida, Decomposition and interception of long waves by a submerged horizontal plate, Coast. Eng. (1990) 1228–1241.
[7] B. Molin, P. Betous, Atténuation de la houle par une dalle horizontale immergée et perforée, in: Quatrièmes journées de l'hydrodynamique, Nantes, France, 1–3 March 1993, pp. 388–400.
[8] J. Brossard, M. Chagdali, Experimental investigation of the harmonic generation by waves over a submerged plate, Coast. Eng. 42 (2001) 277–290.
[9] K. Wang, Z.-Q. Zhang, M.-T. Luan, Flow field analysis of submerged horizontal plate type breakwater, China Ocean Eng. 27 (2013) 821–828.
[10] H. Behera, T. Sahoo, Hydroelastic analysis of gravity wave interaction with submerged horizontal flexible porous plate, J. Fluids Struct. 54 (2015) 643–660.
[11] V. Rey, R. Capobianco, C. Dulou, Wave scattering by a submerged plate in presence of a stead uniform current, Coast. Eng. 47 (2002) 27–34.
[12] H.-X. Lin, D.-Z. Ning, Q.-P. Zou, B. Teng, L.-F. Chen, Current effects on nonlinear wave scattering by a submerged plate, J. Waterw. Port Coast. Ocean Eng. 140 (2014) 04014016.
[13] V. Rey, J. Touboul, Forces and moment on a horizontal plate due to regular and irregular waves in the presence of current, Appl. Ocean Res. 33 (2011) 88–99.
[14] P. Maissa, G. Rousseaux, Y. Stepanyants, Influence of shear-flow vorticity on wave–current interaction, in: 7th International Conference on Coastal Dynamics, Arcachon, France, 2013, pp. 1137–1146.
[15] P. Faltot, R. Bellanger, J. Mougenot, G. Rousseaux, Wave–current interaction: measuring the dispersion relation, in: 8th National Days of Coastal Engineering – Civil Engineering, 2014.